Supplemental Digital Content

Table of Contents

Supplementary Materials and Methods

Animals

This study complies with the ARRIVE guidelines and the Charité animal welfare guidelines. The experimental protocols were approved by the State Office of Health and Social Affairs of Berlin (G0264/14 & T0096/02). Before experiments, the animals had at least seven days for acclimation in our animal shed. The accommodation was in groups of two with food *ad libitum* and a 12-h light on/light off cycle.

Slice preparation, electrophysiology, and induction of seizure-like events and spreading depolarization ex vivo

For experiments in cortical slices, 34 Wistar rats (22 males and 12 females, weight: 250-300 g, age: ~8 weeks) were sacrificed. Coronal slices containing frontal cortex were stored in an

interface chamber and perfused with artificial cerebrospinal fluid (CSF) containing (in mM): 129 NaCl, 26 $NaHCO_3$, 10 glucose, 3 KCl, 1.25 NaH_2PO_4, 1.6 $CaCl_2$, and 1.8 $MgCl_2$ (flow 2 ml/min). Experiments were started after two hours of recovery following slicing. For population spike generation, single electrical stimuli were applied with a bipolar electrode in the white matter. Recordings of field potentials and changes in $[K^+]_o$, $[Na^+]_o$, or $[Ca2^+]_o$ were performed with double-barreled ion-sensitive microelectrodes, manufactured, and tested as previously described [1]. Ionophore cocktails (Potassium Ionophore I 60031, Sodium Ionophore II 71178, or Calcium Ionophore I 21048) were provided all from Fluka, Buchs, Switzerland.

Seizure-like events were induced by continuous perfusion of Mg^{2+}-free artificial CSF (without $MgCl_2$ but similar ion concentrations as described above) during 40-60 min until stable seizure-like events were established. Spreading depolarization was induced by repeated local application of 3 M KCl with a glass micropipette before, during, and after treatment with isoflurane.

Drugs

In brain slices experiments, isoflurane was applied with a calibrated vaporizer (Drager, Germany) in a mixture with carbogen (flow 1 l/min). Isoflurane output was controlled with a Vamos® monitor (Dräger, Germany). Accordingly, the calculated concentrations of isoflurane in the solution were 0.24 mM for 1% and 0.72 mM for 3% isoflurane (using the water/gas partition of Bunsen (α) at 37°C) [2]. In experiments concerning the effects of isoflurane on interstitial ion changes in the absence of synaptic activity and under blockade of 2-pore domain K^+ channels, tetrodotoxin (1 µM), amlodipine besylate (50 µM), and doxapram hydrochloride (50 µM) were applied with artificial CSF (Sigma-Aldrich, Germany). In *in vivo* experiments concerning the effects of mild Na^+/K^+-ATPase inhibition, 10 µM ouabain octahydrate (Sigma-Aldrich, Germany) was solved in artificial CSF and continuously applied to the open cranial window.

Na^+/K^+-ATPase activity assay

To measure the effect of isoflurane on actual Na^+/K^+-ATPase activity, we performed a coupled enzyme assay as previously described (Figure 3) [3, 4]. In short, acute brain slices were prepared as described above and allowed to equilibrate for 120 min after slicing, and then exposed to carbogen with or without 3% isoflurane gas for 60 min in an interface-type recording chamber. The slices were collected, flash-frozen in liquid nitrogen, and homogenized. Tissue was then homogenized in 10 ml solution per 1 g wet weight containing 0.25 M sucrose, 1.25 mM EGTA, and 10 mM Tris, pH 7.0, at 25°C, by eight strokes in a precooled PTFE-glass Potter-Elvehjem homogenizer. The brain homogenate was centrifuged at 750 g for 5 minutes (4°C). Analysis of Na^+/K^+-ATPase activity was performed on the supernatant without further dilution. Stock solutions of reaction buffer (with 10 µM, 10 mM, or without ouabain), auxiliary enzymes, and substrates were prepared in advance. The final reaction mixture contained 125 mM Tris buffer, 1 mM EGTA, 120 mM NaCl, 12.5 mM KCl, 5 mM NaN_3, 5 mM $MgCl_2$, 5 mM ATP, 2.5 mM phosphoenolpyruvate, 0.5 mM NADH, and 15 units each of lactate dehydrogenase (type XI) and pyruvate kinase (type III). Brain homogenate samples, auxiliary enzymes, and substrates were added to the reaction buffer stock solutions omitting only ATP. The mixture was preincubated for 5 min at 37°C in the reading compartment of temperature-controlled Infinite 200 PRO (Tecan, Männerdorf, Switzerland) at 37°C. The reaction was initiated by adding 10 µl of ATP-Na_2 solution to each well.

The enzyme assay couples the formation of adenosine diphosphate by ATPases to NADH oxidation in the presence of excess pyruvate kinase, lactate dehydrogenase, and

phosphoenolpyruvate. The assay measures the rate of NADH absorbance decrease, which is proportional to the rate of steady-state ATP hydrolysis. NADH oxidation was continuously monitored spectrophotometrically at 340 nm in the presence and absence of ouabain. ATPase activity was calculated from the slope of the linear portion of the tracing, the NADH millimolar extinction coefficient, the volume of the reaction mixture, and the total amount of protein in the reaction mixture. The Na^+/K^+-ATPase activity represents the ouabain-suppressible portion of total ATPase activity. To distinguish between α1 and α2/3 isoforms of the Na^+/K^+-ATPase different concentrations of ouabain (10 mM and 10 µM, respectively) were present in the reaction mixture.

Additionally, to test for unspecific effects of isoflurane, such as modification of lipid bilayer properties, we performed an independent run where we added isoflurane in liquid form to the reaction mixture of untreated control whole brain homogenates to achieve isoflurane concentrations that far exceed the clinical application (1 and 3 vol%).

In vivo preparation, electrophysiology recordings, isoflurane titration, and characterization of hypnotic depth

20 male Wistar rats (~250 g, ~8 weeks) were first anesthetized with isoflurane and nitrous oxide (1.5% and 70% respectively) in an induction chamber (15 animals were included in the analysis, five animals were excluded as described below). Nitrous oxide was shortly applied during anesthesia induction (3-5 minutes) to avoid high concentrations of isoflurane before electrophysiological recordings and to minimize pain during local infiltration with lidocaine. After induction, anesthesia was exclusively maintained with 1-2% isoflurane with a mask. Thereafter, anesthesia was maintained with 1-2% isoflurane through a nares mask. Pulse oximetry was monitored (MouseOxplus, Starr Life Sciences, Oakmont, USA) during the surgical procedure (total duration of preparation procedure was ~60±20min). Body temperature was maintained at 37.0±0.5°C (Harvard Apparatus, Holliston, USA). Animals were mechanically ventilated after tracheotomy (Harvard Small Animal Ventilator 683, Holliston, USA) and end-tidal carbon dioxide was maintained at ~35 mmHg. Blood pressure was monitored after cannulation of the femoral artery. For hydration, 8-10 ml saline per kg body weight per hour were infused. A mini craniotomy in the frontal region 2 mm from the sagittal suture and 2 mm from the coronal suture was performed after fixation in a stereotaxic system. To avoid stress, all skin incisions were performed after local infiltration with 0.1-0.3 ml lidocaine 1% (Brown, Germany). A chamber was formed with bone cement around the craniotomy for perfusion with artificial CSF containing (in mM) NaCl 127.5, KCl 3.0, $CaCl_2$ 1.5, $MgSO_4$ 1.2, $NaHCO^-_3$ 24.5, glucose 3.7, and urea 6.7, and was gassed with 50% O_2 and 3-4% CO_2. After a small dura incision, an ion-sensitive microelectrode and a stimulation electrode (if corresponding) were inserted into the frontal cortex at ca. 100 µm depth from the brain surface. Following registration of phase 2 anesthesia (alpha/delta band, 0-12 Hz) in the electrocorticography, isoflurane was titrated (from 1-1.5% to 2.5-3.5%) to establish a burst suppression pattern. Complementary to electrocorticography, a pinching test was performed and quantified (1, strong flexion; 2, weak flexion; 3, no flexion observed) at regular time points to check for anesthesia depth clinically. Animals were sacrificed under deep anesthesia. Brains were removed and frozen at -80°C for future analysis. For experiments on stimulus-induced $[K^+]_o$ increases (group 1, total number of animals = 6; two animals excluded due to surgical complications), a bipolar stimulation electrode was placed in the cortex ~2 mm from the recording electrodes (stimulation parameters: 20 Hz, 2 s, 5 V). For experiments concerning changes in $[K^+]_o$ baseline (group 2), a total of seven animals were recorded, and one animal was excluded due to ventilation problems. Effects of ouabain during phase 2 of general anesthesia were studied in five animals (group 3, total number of animals = 7; two animals excluded due to cortical

spreading depolarization during recordings). In four animals (group 2), data concerning changes in tissue partial oxygen pressure and changes in regional cerebral blood flow during burst suppression anesthesia were recorded and published in Berndt *et al.*, 2021 [5].

Supplementary Table 1. Monitoring Data Group 1 (effects of Isoflurane on $[K^+]_o$ clearance). MAP: mean arterial pressure; $ETCO_2$: end-tidal carbon dioxide.

		MAP (mmHg)	Oxygen saturation (%)	$ETCO_2$ (mmHg)	Respiratory rate/min	Rectal temperature	Pinching test*	n
Phase 2	10'	82.0±9.7	99.7±0.6	37.6±4.1	80.6±13.2	37.0±0.0	2/3	4
	20'	82.7±8.2	99.7±0.6	38.3±4.4	74.9±17.7	37.0±0.0	2/3	4
Burst suppression	30'	82.1±5.5	99.7±0.5	38.1±4.2	74.7±17.3	37.0±0.0	3/3	4
	40'	83.0±4.0	99.7±0.5	38.2±4.5	74.3±18.1	37.0±0.0	3/3	4
	50'	83.4±4.3	99.7±0.5	37.9±4.5	75.2±17.9	37.0±0.0	3/3	4
	60'	83.2±3.4	99.7±0.5	37.4±4.2	78.4±15.2	37.0±0.0	3/3	4
	70'	80.3±8.4	99.7±0.5	35.0±1.9	86.3±9.4	37.0±0.0	3/3	4
	80'	83.1±1.8	99.7±0.5	38.0±4.2	74.5±17.2	37.0±0.0	3/3	4
	90'	81.5±10.3	99.7±0.5	34.6±2.0	86.1±8.9	37.0±0.0	3/3	4
	100'	81.7±12.1	99.7±0.5	34.5±2.2	85.6±9.8	37.0±0.0	3/3	4
	110'	87.0±8.6	99.7±0.6	34.6±2.0	86.3±9.3	37.0±0.0	3/3	4

*Pinching test: 1, strong flexion; 2, weak flexion; 3, no flexion observed.

Supplementary Table 2. Monitoring Data Group 2 (isoflurane effects on $[K^+]_o$ baseline)

		MAP (mmHg)	Oxygen saturation (%)	$ETCO_2$ (mmHg)	Respiratory rate/min	Rectal temperature	Pinching test*	n
Phase 2	10'	80.5±9.1	98.5±1.3	34.6±1.2	86.3±8.6	36.9±0.0	2/3	6
	20'	81.1±10.2	98.3±1.7	35.0±1.8	85.7±11.8	37.0±0.0	2/3	6
Burst suppression	30'	83.1±9.4	98.7±1.1	35.4±2.6	90.7±12.1	37.0±0.0	2/3	6
	40'	80.9±8.5	98.5±1.2	35.5±2.4	86.6±10.0	37.0±0.0	3/3	6
	50'	78.6±7.0	98.5±1.3	34.9±2.1	83.5±11.8	37.0±0.0	3/3	6
	60'	80.7±7.4	98.5±1.4	35.0±1.9	83.2±13.4	37.0±0.0	3/3	6
	70'	76.1±5.8	98.4±1.	34.8±0.8	87.2±9.3	37.0±0.0	2/3	6
	80'	84.3±8.2	98.6±1.2	35.4±2.7	89.6±10.2	37.0±0.0	3/3	6
	90'	77.6±5.9	98.3±1.0	35.9±2.8	87.9±7.5	37.0±0.0	3/3	6
	100'	77.4±5.7	98.1±1.2	35.6±2.4	84.4±9.6	37.0±0.0	3/3	6
	110'	75.±5.81	98.0±1.2	35.9±1.4	80.2±16.8	37.0±0.0	3/3	6

*Pinching test: 1, strong flexion; 2, weak flexion; 3, no flexion observed.

Supplementary Table 3. Monitoring Data Group 3 (effects of ouabain during Phase 2 anesthesia)

		MAP (mmHg)	Oxygen saturation (%)	$ETCO_2$ (mmHg)	Respiratory rate/min	Rectal temperature	Pinching test*	n
Control	**10' phase 2**	80.1±16.0	99.0±0.7	36.3±2.5	84.9±7.4	36.9±0.0	2/3	5
	20' phase 2	78.9±12.2	97.9±2.9	36.2±2.6	89.5±6.9	37.0±0.0	2/3	5
Ouabain	**30' phase 2**	80.4±10.4	99.2±0.8	35.4±1.6	91.1±15.2	37.0±0.0	2/3	5
	40' phase 2	80.0±12.4	99.2±0.7	35.3±1.1	83.3±8.8	37.0±0.0	2/3	5
	50' phase 2	78.9±7.9	98.9±0.7	35.1±1.3	83.7±8.4	37.0±0.0	3/3	5
	60' phase 2	77.4±5.8	98.4±1.4	35.1±1.3	84.8±10.1	37.0±0.0	3/3	5
	70' phase 2	78.9±6.7	97.8±0.5	34.9±1.3	86.6±11.0	37.0±0.0	3/3	5

*Pinching test: 1, strong flexion; 2, weak flexion; 3, no flexion observed

Biophysical computational model

We used an adaptation of the electrophysiological model by Berndt *et al.* [6, 7]. The model describes the dynamics of the intra- and extracellular concentrations of the three ion species Na^+, K^+, and Cl^-, together with the membrane potential V.

Changes in ion concentrations in the extracellular space and the cellular lumen result from the passive electro-diffusive movement of ions through voltage-dependent and voltage-independent ion channels in the plasma membrane as well as active (ATP-dependent) transport of ions through the plasma membrane by the Na^+/K^+-ATPase.

Passive transport of ions across the membrane includes basal leak currents I_X^p described by basal permeabilities and ion currents through voltage-gated channels (Na^+, K^+) described through the gated permeabilities $P_{Na/K}^g$. Excitation is achieved by the opening of ligand-gated sodium channels (i.e. increase of the excitatory sodium permeability P_{Na}^{exc}).

The model describes the time-dependent variation of the three ion species Na^+, K^+, and Cl^-. The change in cellular ion concentrations $[X]_{cell}$ due to ion fluxes I_x is given by

$$\frac{d[X]_{cell}}{dt} = -\frac{I_X}{z_X \cdot F \cdot Vol_{cell}} \quad (1)$$

Here, z_X is the charge of ion species X and F the Faraday constant. The change in the external ion concentrations $[X]_{out}$ due to ion fluxes I_x is given by

$$\frac{d[X]_{out}}{dt} = \frac{I_X}{z_X \cdot F \cdot Vol_{ext}} \quad (2)$$

The ion currents I_x are the sum of the passive current I_X^a and the active current I_X^p

$$I_x = I_X^a + I_X^p \quad (3)$$

The passive current I_X^p describes the electro-diffusion of ions across the cell membrane and is modeled via the Goldman-Hodgkin-Katz equation

$$I_X^p = A \cdot P_X \cdot U \cdot F \cdot z_X^2 \frac{[X]_{cell} \cdot \exp(z_X \cdot U) - [X]_{out}}{1 - \exp(z_X \cdot U)} \tag{4}$$

Here, A is the surface of the cell membrane and U is defined by

$$U = \frac{V \cdot F}{1000 \cdot R \cdot T} \tag{5}$$

with V being the membrane potential, R the universal gas constant, T the temperature, and 1000 the scaling factor as the membrane potential is given in mV. The total permeability for the ion species X and P_X is the sum of the permeability of the basal channels P_X^0, the permeability of the voltage-gated channels P_X^g, and the permeability of the excitatory channels P_X^{ex}

$$P_X = P_X^0 + P_X^g + P_X^{exc} \tag{6}$$

The voltage-gated channels for Na^+ and K^+ are described by the standard model of Hodgkin and Huxley

$$P_K^g = m^4 \cdot P_K^{g0} \tag{7}$$

$$P_{Na}^g = n^3 \cdot h \cdot P_{Na}^{g0} \tag{8}$$

where the gating variables $g \in \{m, n, h\}$ obey the ordinary differential equation

$$\frac{dg}{dt} = C_g\left(\alpha_g(1 - g) + \beta_g \cdot g\right) \tag{9}$$

with $C_g$being a constant and α_g and $\beta_g$being voltage-dependent functions.

The active transport of ions by the Na^+/K^+-ATPase is given by

$$I_{NaKATPase}^a = V_{max}^{NaKATPase} \cdot A \cdot \left(\frac{Na_{cyt}^{n_{Na}}}{Na_{cyt}^{n_{Na}} + {K_0}_{Na}^{n_{Na}}}\right) \cdot \left(\frac{K_{ext}^{n_K}}{K_{ext}^{n_K} + {K_0}_K^{n_K}}\right) \tag{10}$$

$n_{Na} = 3$ [8]

$K_{0_{Na}} = 12.8$ [8]

$n_K = 1.6$ [9]

$K_{0_K} = 4.3$ [9]

The membrane is modeled as a capacitor with total capacitance C related to specific capacitance c_m and total charge Q via

$$C = c_m A = \frac{Q}{V} \tag{11}$$

Differentiation for time gives

$$\frac{dV}{dt} = \frac{1}{C}\frac{dQ}{dt} - \frac{Q}{C^2}\frac{dQ}{dt} \tag{12}$$

Given that the membrane capacity is constant, $\frac{dC}{dt} = 0$, and

$$\frac{dV}{dt} = \frac{1}{C}\sum_X \frac{dQ_X}{dt} = \frac{1}{C}\sum_X I_X \quad (13)$$

Parameters and constants

Supplementary Table 4. Constants.

Name	Value	Unit	Description
T	293	K	Temperature
R	8.3	$\frac{J}{mol \cdot K}$	Universal gas constant
F	96490	$\frac{C}{mol}$	Faraday's constant

Supplementary Table 5. Geometry.

Name	Value	Unit	Description
r_0	10^{-6}	m	Cell radius
l_0	$15 \cdot 10^{-6}$	m	Cell length
A	$2 \cdot l_0 \cdot \pi \cdot r_0$	m^2	Cell surface
Vol_{cell}	$l_0 \cdot \pi \cdot r_0^2$	m^3	Cell volume
Vol_{ext}	$0.3 \cdot Vol_{cell}$	m^3	External volume

Supplementary Table 6. Initial ion concentration.

Name	Value	Unit	Reference	Description
$[Cl]_{cell}$	8	mM	[10]	Bulk Cl^- concentration
$[K]_{cell}$	140	mM	[10]	Bulk K^+ concentration
$[Na]_{cell}$	10	mM	[10]	Bulk Na^+ concentration
$[Cl]_{óut}$	150	mM	[10]	External Cl^- concentration
$[K]_{out}$	4	mM	[10]	External K^+ concentration
$[Na]_{out}$	145	mM	[10]	External Na^+ concentration

Supplementary Table 7. Capacitance and voltage.

Name	Value	Unit	Equations	Reference	Description
c_m	10^{-6}	$\frac{F}{m^2}$	(11)	[11]	Specific membrane capacitance
V	-70	mV	(5), (11)	[12]	Membrane potential
C	$c_m \cdot A$	F	(11), (12), (13)	-	Total capacitance
Q	-	C	(11), (12)	-	Excess charge

Supplementary Table 8. Hodgkin-Huxley transition rates.

g	C_g	α_g	β_g
m	1000	$\frac{0.1-0.01(V+65)}{\exp(1-0.1(V+65)-1)}$	$0.125\exp\left(\frac{-(V+65)}{80}\right)$
n	1000	$\frac{2.5-0.01(V+65)}{\exp(2.5-0.1(V+65)-1)}$	$4.0\exp\left(\frac{-(V+65)}{18}\right)$
h	1000	$0.07\exp\left(\frac{-(V+65)}{20}\right)$	$\frac{1}{\exp((30-(V+65))/10)+1}$

Supplementary Table 9. Permeabilites.

Name	Value	Unit	References	Description
P_{Cl}^0	$40 \cdot 10^{-9}$	$\frac{m}{s}$	[10, 13]	Basal chloride permeability
P_K^0	$20 \cdot 10^{-9}$	$\frac{m}{s}$	[10, 12]	Basal potassium permeability
P_{Na}^0	$1.2 \cdot 10^{-9}$	$\frac{m}{s}$	[10, 12, 13]	Basal sodium permeability
P_K^g	$750 \cdot 10^{-9}$	$\frac{m}{s}$	[14]	Gated potassium permeability
P_{Na}^g	$225 \cdot 10^{-9}$	$\frac{m}{s}$	[14]	Gated sodium permeability

Data Analysis and Statistics

To reduce subjective bias and other systematic errors of technical nature, we randomized animal order and slice placement location. To generate random, uniformly distributed integers without replacement, we employed a custom-written Python function based on a pseudo-random number generator implementation from the Python standard library (random, v. 3.8.3). Animals were randomized per cage to determine the order of experiments for all experimental paradigms (*in vivo*, acute brain slices, enzyme assay). In acute brain slices experiments, the allocation of slices to the available space in the recording chamber was randomized. In addition, we identified coronal slicing planes according to a neuroanatomical rat brain atlas and only employed brain slices from similar slicing planes for identical protocols to minimize the potential confounding effects of varying slicing planes.

Analyses of brain slice data were blinded and carried out by a different researcher using a batch processing approach of electrophysiological files carrying nondescript names. The sequence of samples for Na^+/K^+-ATPase assay measurements was randomized. Both measurement and data analysis of absorbance changes were blinded and carried out by different team members. Blinding could not be applied in acute brain slice experiments with the application of tetrodotoxin, doxapram, and amlodipine due to a shortage of personnel.

Sample sizes necessary for the comparison of the differences of two dependent means in a matched pairs design *in vivo* experiments were calculated using G*Power (v. 3.1.9.2). Based on our previous experience with the isoflurane effects during phase 2 and burst suppression anesthesia we set the effect size (Cohen's d) to 1.2. Power was set to 80%, we assumed a normal distribution, chose paired two-tailed t-tests and arrived at 7-8 animals per group. Sample

sizes for acute brain slice experiments and the ATPase activity assay were estimated based on our previous experience. Based on the sample size calculation and the experimental designs, we intended to collect at least seven observations (animals, slices) per condition. A summary of all sample sizes is available in the Supplementary Results Tables.

A total of five animals had to be excluded from the analysis of the *in vivo* experiments: two rats were excluded due to the occurrence of spreading depolarizations following cortical ouabain application, one rat due to ventilation issues, and two rats because of complications during the surgery. We had to exclude eleven brain slices based on poor viability during the initial testing in the interface chamber.

Data Acquisition and Analysis

Analog signals were digitalized with Power1401 and recorded with Spike2 (Cambridge Electronic Design Limited, Cambridge, UK). Data analysis and statistics were performed using Spike2, Origin software (Version 6, Microcal Software, Northampton, MA, USA), and SPSS v.20.0 (IBM Corporation, Armonk, NY, USA).

Ex vivo, absolute amplitudes of stimulus-induced population spikes were measured with Spike2 software (Cambridge Electronic Design Limited, Cambridge, UK), and $[K^+]_o$, $[Na^+]_o$, and $[Ca^{2+}]_o$ were calculated using a modified Nernst's equation as described previously [1]. Incidence, duration, amplitude, and the number of spikes per seizure-like event were quantified for at least ten bursts during a baseline period of 20 minutes followed by the treatment with 1% and 3% isoflurane. $[K^+]_o$ increases per seizure-like event, $T1_{50}$, and $T2_{50}$ (calculated as described below) were analyzed to assess K^+ clearance. Spreading depolarization properties were assessed by comparing the absolute amplitude and duration of the field potential direct current shifts and spreading depolarization-associated changes in $[K^+]_o$ and in $[Na^+]_o$. To monitor the restoration of $[K^+]_o$ and $[Na^+]_o$ during spreading depolarization and seizure-like events, $T1_{50}$ and $T2_{50}$ were measured after the ion plateau as well.

In vivo, electrocorticography and related changes in absolute $[K^+]_o$ and $[K^+]_o$ clearance were measured and analyzed using Spike2 (Cambridge Electronic Design Limited, Cambridge, UK). We estimated $[K^+]_o$ clearance by measuring the time of $[K^+]_o$ decay after stimulation during two distinct periods: an early decay time (first half decay from maximal amplitude or $T1_{50}$) and a late decay time (second half decay from maximal amplitude or $T2_{50}$). To minimize burst-associated distortion of K^+ curves, stimulation was performed during suppression. Furthermore, $T2_{50}$ was sometimes measured before the return to the baseline before stimulation if burst-associated $[K^+]_o$ were registered. Early and established burst suppression stages (first 10 minutes and up to 40 minutes, respectively) were characterized by analyzing burst amplitude of electrocorticography, burst interval, and characteristics of $[K^+]_o$ increases per burst (absolute $[K^+]_o$ increase per burst and slope of $[K^+]_o$ clearance within a burst). To ensure accurate $[K^+]_o$ quantification, ion-selective microelectrodes were tested once more after completing the recording using artificial CSF containing 3 mM K^+. In experiments concerning the effects of ouabain during phase 2 anesthesia, the total power of bursting activity over time was calculated using the power spectrum function of the Matlab Signal Processing Toolbox (Mathworks, Natick, MA).

Supplementary Results Tables

Supplementary Table 10. Changes in $[K^+]_o$ and $[Na^+]_o$ baseline during 1% and 3% isoflurane in brain slices. n: number of slices; N: number of animals. Shading colors apply for data from male (blue), and female (orange) Wistar rats, and integrations of both sexes (green).

	Control mean±SD	1% isoflurane mean±SD	3% isoflurane mean±SD	Washout mean±SD	p-values				n	N
					Control versus 1%	Control versus 3%	Control versus washout	3% versus washout		
$[K^+]_o$ [mM]	3.0±0.0	3.2±0.2	4.0±0.7	2.9±0.3	0.007	<0.001	0.488	<0.001	22	7
[K+]o [mM]	3.0±0.1	4.2±0.1	3.9±0.3	3.0±0.2	0.010	<0.001	0.545	<0.001	17	6
$[K^+]_o$ [mM]	3.0±0.1	3.2±0.1	4.0±0.5	3.0±0.2	<0.001	<0.001	0.827	<0.001	39	13
$[Na^+]_o$ [mM]	153.3±1.0	149.2±5.3	142.7±8.4	149.8±9.3	0.089	<0.001	0.182	0.008	11	6
$[Na^+]_o$ [mM]	153.5±0.7	151.4±1.5	146.9±3.0	151.5±3.4	<0.012	<0.001	0.184	<0.001	17	6
$[Na^+]_o$ [mM]	153.4±0.8	150.6±3.5	145.2±6.0	150.9±6.1	<0.192	<0.012	0.0409	<0.078	28	12
Population spike amplitude [mV]	1.29±0.76	1.05±0.823	0.59±0.45	0.90±0.56	0.029	<0.001	0.014	<0.001	20	6
Population spike amplitude [mV]	1.23±0.59	1.13±0.68	0.65±0.39	0.92±0.46	0.101	<0.001	0.014	<0.006	17	6
Population spike amplitude [mV]	1.21±0.68	1.08±0.75	0.62±0.42	0.91±0.51	0.005	<0.001	<0.001	<0.001	37	12

Supplementary Table 11. Effects of 3% isoflurane in interstitial $[K^+]_o$, $[Na^+]_o$, and $[Ca^{2+}]_o$ in the presence of Tetrodotoxin, amlodipine, and doxapram. n: number of slices; N: number of animals. Shading colors apply for data from male (blue), and female (orange) Wistar rats, and integrations of both sexes (green).

	Control mean±SD	3% isoflurane mean±SD	Washout mean±SD	p-values			n	N
				Control versus 3%	Control versus washout	3% versus washout		
$[K^+]_o$ [mM]	3.0±0.0	4.2±0.6	2.9±0.3	<0.001	0.194	<0.001	8	3
$[K^+]_o$ [mM]	3.0±0.0	4.1±0.5	3.4±0.8	0.004	0.382	0.014	10	4
$[K^+]_o$ [mM]	3.0±0.0	4.2±0.6	3.2±0.6	<0.001	0.509	<0.001	18	7
$[Na^+]_o$ [mM]	153.9±0.7	146.6±2.7	150.0±2.7	0.001	0.0103	0.004	8	3
$[Na^+]_o$ [mM]	153.5±1.1	144.7±1.6	150.8±1.7	0.010	0.196	0.089	10	4
$[Na^+]_o$ [mM]	153.7±1.0	145.6±4.2	150.4±4.0	<0.001	0.0257	0.0115	18	7
$[Ca^{2+}]_o$ [mM]	1.60±0.0	1.2±0.1	1.3±0.2	<0.001	0.044	0.168	6	3
$[Ca^{2+}]_o$ [mM]	1.6±0.0	1.2±0.1	1.5±0.1	<0.001	0.017	0.003	10	4
$[Ca^{2+}]_o$ [mM]	1.6±0.0	1.2±0.1	1.3±0.2	<0.001	0.002	0.001	16	7

Supplementary Table 12. Effects of 1% and 3% isoflurane on seizure-like events (SLE) in rat brain slices.

	Control mean±SD	1% isoflurane mean±SD	3% isoflurane mean±SD	p-values			n	N
				Control versus 1%	Control versus 3%	1% versus 3%		
Incidence [SLE/min]	9.20±2.97	3.45±0.93	1.24±0.51	0.029	<0.001	0.029	11	4
Incidence [SLE/min]	10.46±1.73	4.54±1.56	0.93±0.50	<0.001	<0.001	<0.001	10	4
Incidence [SLE/min]	9.80±2.49	3.97±1.36	1.09±0.52	0.002	<0.001	<0.002	21	8
Duration [s]	1.7±0.8	3.5±1.3	4.3±0.8	0.007	0.003	0.529	11	4
Duration [s]	1.6±0.5	4.1±1.4	5.5±0.5	0.023	0.002	0.196	10	4
Duration [s]	1.76±0.6	3.9±1.2	4.9±0.9	<0.001	<0.001	0.172	21	8
$\Delta[K^+]_o$/SLE [mM]	2.5±1.5	3.9±1.9	3.6±1.9	<0.001	0.069	0.028	11	4
$\Delta[K^+]_o$/SLE [mM]	2.5±1.5	3.5±2.0	5.0±2.0	0.06	<0.001	0.016	10	4
$\Delta[K^+]_o$/SLE [mM]	2.5±1.5	3.7±2.0	4.3±2.0	<0.001	<0.001	0.080	21	8
$T1_{50}$ [s]	1.6±0.6	2.6±1.6	3.9±2.3	0.029	<0.001	0.003	11	4
$T1_{50}$ [s]	1.4± 0.4	2.2± 0.7	3.8± 1.2	0.038	0.001	0.040	10	4
$T1_{50}$ [s]	1.5± 0.5	2.5± 1.2	3.8± 1.9	0.002	<0.001	0.004	21	8
$T2_{50}$ [s]	3.7±2.4	11.9±3.8	22.1±7.0	0.029	<0.001	0.030	11	4
$T2_{50}$ [s]	4.4± 2.6	10.6± 3.2	23.3±6.6	0.129	0.001	0.026	10	4
$T2_{50}$ [s]	4.1± 2.6	11.2± 3.5	22.7±6.6	0.008	0.001	0.01	21	8
Spikes/SLE	15.04±12.09	34.92±12.39	42.79±10.09	0.005	0.005	0.083	10	4
Spikes/SLE	12.01±1.61	23.65±7.89	42.25±11.20	0.038	<0.001	0.040	10	4
Spikes/SLE	13.53±8.54	29.28±11.65	42.52±10.38	<0.001	<0.001	0.122	21	8

Supplementary Table 13. Effects of 1% and 3% isoflurane on spreading depolarization in brain slices. n: number of slices; N: number of animals. Shading colors apply for data from male (blue), and female (orange) Wistar rats, and integrations of both sexes (green).

	Control mean±SD	1% isoflurane mean±SD	3% isoflurane mean±SD	Washout mean±SD	p-values			n	N
					Control versus 1%	Control versus 3%	1% versus 3%		
Amplitude spreading depolarization [mV]	-19.06±9.24	-20.70±9.79	-15.25±10.14	-24.29±9.88	0.459	0.793	0.145	7	4
Amplitude spreading depolarization [mV]	-18.6±4.28	-19.17±5.95	-16.07±6.51	-24.56±8.45	0.755	0.340	0.0.036	7	4
Amplitude spreading depolarization [mV]	-18.83±6.92	-19.94±7.83	-15.66±8.19	-24.34±8.84	0.575	0.401	0.302	14	8
Duration [s]	41.1±7.2	59.2±12.7	126.9±54.3	55.0±8.9	0.085	0.008	0.086	7	4
Duration [s]	46.7±14.2	66.2±15.9	113.05±48.0	54.1±17.0	0.032	0.023	0.033	7	4
Duration [s]	43.9±11.2	62.7±14.3	112.0±49.8	54.8±8.0	0.013	<0.001	0.014	14	8
$\Delta[K^+]_o$/ spreading depolarization [mM]	31.6±6.5	30.1±5.4	20.8±5.7	30.3±6.4	0.438	0.005	0.015	7	4

$\Delta[K^+]_o$/ spreading depolarization [mM]	33.9±14.2	33.2±14.7	24.6±11.7	26.7±15.8	0.803	0.062	0.029	7	4
$\Delta[K^+]_o$/ spreading depolarization [mM]	32.7±10.7	31.7±10.8	22.7±9.1	29.7±5.9	0.485	<0.001	<0.001	14	8
$[K^+]_o$ $T1_{50}$ [s]	14.7±4.9	18.1±5.8	31.4±13.7	22.3±8.1	0.085	0.008	0.085	7	4
$[K^+]_o$ $T1_{50}$ [s]	16.5±5.2	21.6±8.5	31.8±13.8	21.1±4.3	0.202	0.099	0.099	7	4
$[K^+]_o$ $T1_{50}$ [s]	15.6±4.9	19.8±7.2	31.7±13.2	22.0±6.8	0.031	<0.001	0.069	14	8
$[K^+]_o$ $T2_{50}$ [s]	51.5±10.7	78.2±22.7	200.1±80.7	121.3±86.2	0.085	0.008	0.008	7	4
$[K^+]_o$ $T2_{50}$ [s]	75.4±16.6	92.1±46.3	192.4±90.5	63.7±17.5	0.380	0.013	0.037	7	4
$[K^+]_o$ $T2_{50}$ [s]	63.43±18.3	85.19±35.8	196.26±82.5	104.87±76.2	0.031	<0.001	0.013	14	8
$\Delta[Na^+]_o$/ spreading depolarization [mM]	-50.1±17.2	-56.3±15.6	-53.6±14.5	-62.7±15.1	0.149	0.615	0.615	7	4
$\Delta[Na^+]_o$/ spreading depolarization [mM]	-57.6±21.3	-58.3±19.2	-34.0±15.4	-35.7±10.4	0.823	0.049	0.049	7	4
$\Delta[Na^+]_o$/ spreading depolarization [mM]	-53.9±19.0	-57.3±16.8	-43.1±17.6	-55.0±18.6	0.265	0.151	0.002	14	8
$[Na^+]_o$ $T1_{50}$ [s]	11.3±5.2	13.9±6.0	20.2±7.4	18.7±3.3	0.0944	0.014	0.078	7	4
$[Na^+]_o$ $T1_{50}$ [s]	13.4±2.3	15.9±4.8	21.9±7.0	14.2±2.5	0.1446	0.034	0.034	7	4
$[Na^+]_o$ $T1_{50}$ [s]	12.4±4.0	14.9±5.3	21.0±7.0	17.4±3.6	0.0189	<0.001	0.002	14	8
$[Na^+]_o$ $T2_{50}$ [s]	25.5±7.0	32.45±0.9	83.5±68.7	32.1±10.1	0.202	0.099	0.099	7	4
$[Na^+]_o$ $T2_{50}$ [s]	29.2±12.1	39.0±16.6	89.7±37.4	26.6±10.5	0.438	0.022	0.049	7	4
$[Na^+]_o$ $T2_{50}$ [s]	27.4±9.7	35.7±13.6	86.6±53.2	30.5±9.7	0.100	0.001	0.047	14	8

Supplementary Table 14. Effects of isoflurane on stimulus-induced neocortical $[K^+]_o$-increases *in vivo* (N=4).

	Phase 2 mean±SD	**Burst suppression mean±SD**	**Evaluated stimuli**	**p-values**
$\Delta[K^+]_o$ [mM]	22.3±1.1	2.3±0.8	(17, 30)	0.9
$T1_{50}$ [s]	3.9±1.1	5.7±1.2	(17, 30)	0.001
$T2_{50}$ [s]	14.0±2.2	30.7±1.0	(17, 30)	0.001

Supplementary Table 15. Baseline $[K^+]_o$ during phase 2 and burst suppression.

		$[K^+]_o$ [mM] (mean±SD)	**N**
Phase 2		3.0±0.1	6
Burst suppression	**10'**	2.7±0.2	6
	20'	2.7±0.6	6
	30'	3.0±0.5	6
	40'	3.2±0.3	6
	50'	3.5±0.4	6
	90'	4.1±0.7	6

Supplementary Table 16. Properties of early and established burst suppression.

	Early burst suppression mean±SD	Established burst mean±SD	N	p-values
Burst amplitude electrocorticography [mV]	0.98±0.46	1.38±0.43	6	0.001
$\Delta[K^+]_o$/burst [mM]	0.3±0.2	0.5±0.2	6	0.022
Slope [$\mu M.^{s-1}$]	-55.4±14.6	-33.5±14.3	6	<0.001
Interval	8.2±2.9	17.0±9.0	6	0.037

Supplementary Results Figures

Supplementary Figures 1 and 2. Sex-specific results of acute brain slice experiments visualized with boxplots displaying data from three groups (female, male, pooled). Boxplots are arranged in columns to facilitate comparison between the corresponding groups and assessment of the general trend. The matching figure of the main document displaying the pooled data is specified at the top.

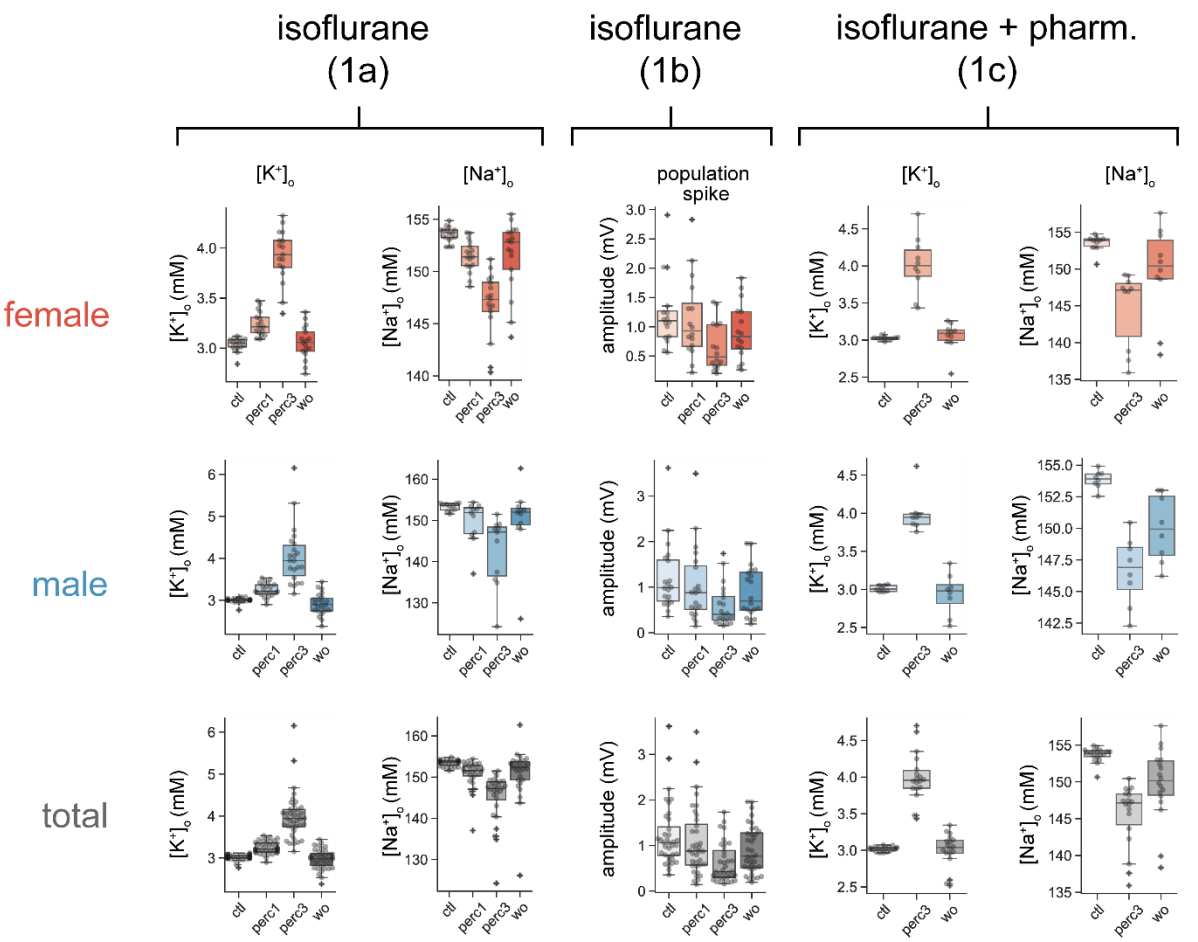
isoflurane (1a)
isoflurane (1b)
isoflurane + pharm. (1c)
female
male
total
$[K^+]_o$
$[Na^+]_o$
population spike
amplitude (mV)
$[K^+]_o$ (mM)
$[Na^+]_o$ (mM)
ctl
perc1
perc3
wo

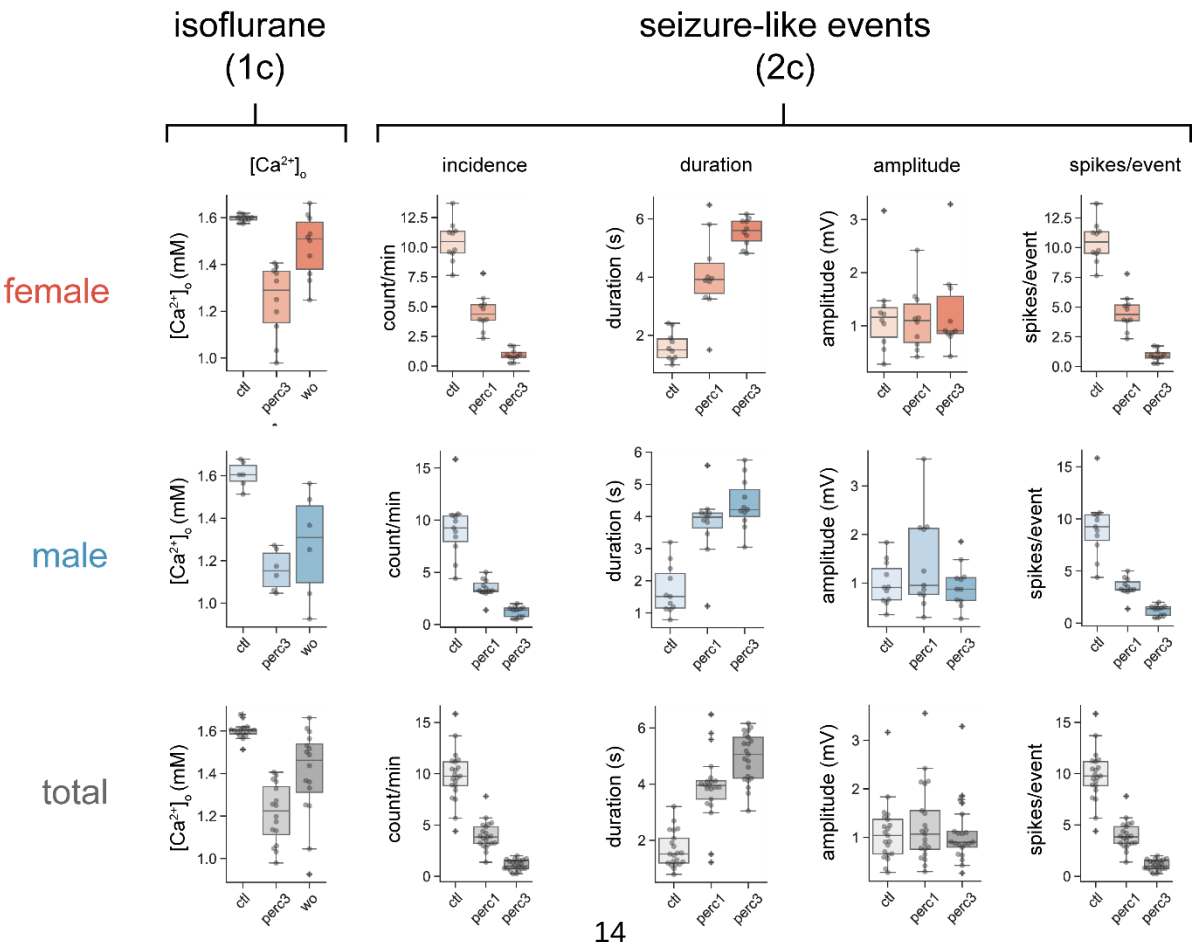
isoflurane (1c)
seizure-like events (2c)
female
male
total
$[Ca^{2+}]_o$
incidence
duration
amplitude
spikes/event
$[Ca^{2+}]_o$ (mM)
count/min
duration (s)
amplitude (mV)
spikes/event
ctl
perc1
perc3
wo

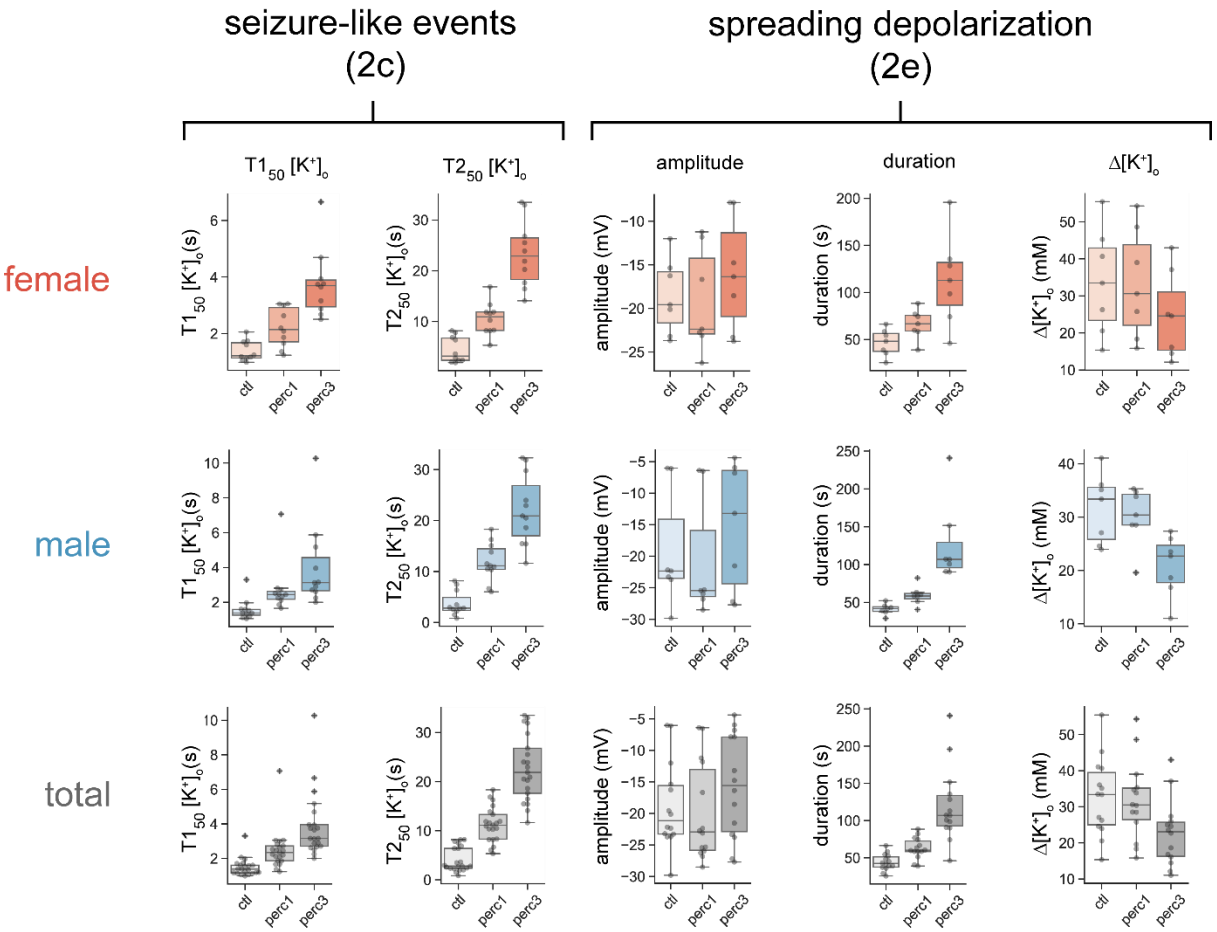
seizure-like events
(2c)
spreading depolarization
(2e)
female
male
total
T1 50 [K+]o
T2 50 [K+]o
amplitude
duration
Δ[K+]o
T1 50 [K+]o (s)
T2 50 [K+]o (s)
amplitude (mV)
duration (s)
Δ[K+]o (mM)
ctl
perc1
perc3

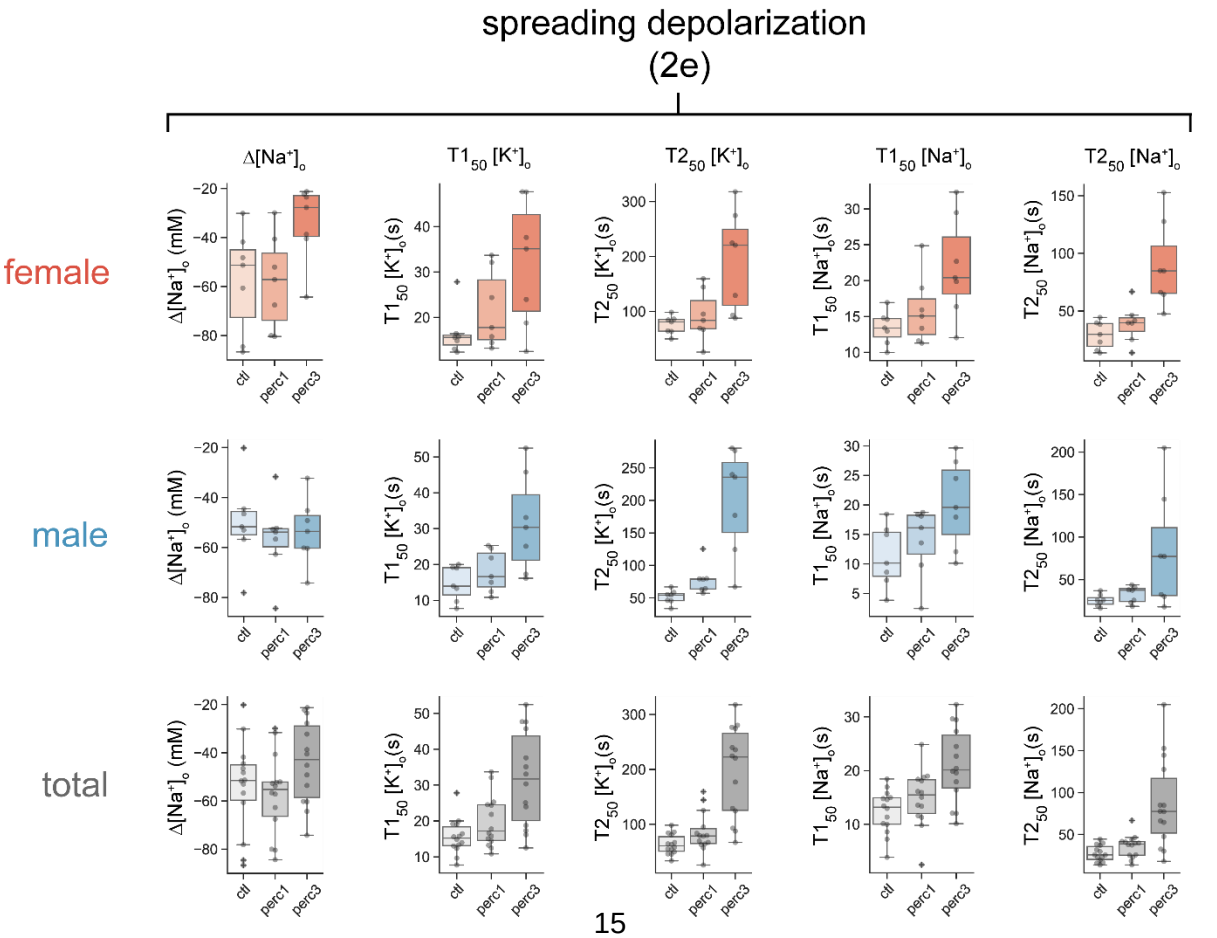
spreading depolarization
(2e)
female
male
total
Δ[Na+]o
T1 50 [K+]o
T2 50 [K+]o
T1 50 [Na+]o
T2 50 [Na+]o
Δ[Na+]o (mM)
T1 50 [K+]o (s)
T2 50 [K+]o (s)
T1 50 [Na+]o (s)
T2 50 [Na+]o (s)
ctl
perc1
perc3

References

1. Liotta, A., et al., *Partial Disinhibition Is Required for Transition of Stimulus-Induced Sharp Wave-Ripple Complexes Into Recurrent Epileptiform Discharges in Rat Hippocampal Slices.* Journal of Neurophysiology, 2011. **105**(1): p. 172-187. DOI: 10.1152/jn.00186.2010.
2. Franks, N.P. and W.R. Lieb, *Selective Actions of Volatile General-Anesthetics at Molecular and Cellular-Levels.* British Journal of Anesthesia, 1993. **71**(1): p. 65-76. DOI: DOI 10.1093/bja/71.1.65.
3. Reiffurth, C., et al., *Na(+)/K(+)-ATPase alpha isoform deficiency results in distinct spreading depolarization phenotypes.* J Cereb Blood Flow Metab, 2020. **40**(3): p. 622-638. DOI: 10.1177/0271678X19833757.
4. Scharschmidt, B.F., et al., *Validation of a Recording Spectrophotometric Method for Measurement of Membrane-Associated Mg- and Nak-Atpase Activity.* Journal of Laboratory and Clinical Medicine, 1979. **93**(5): p. 790-799.
5. Berndt, N., et al., *Low neuronal metabolism during isoflurane-induced burst suppression is related to synaptic inhibition while neurovascular coupling and mitochondrial function remain intact.* Journal of Cerebral Blood Flow and Metabolism, 2021. **41**(10): p. 2640-2655. DOI:10.1177/0271678x211010353.
6. Berndt, N. and H.G. Holzhutter, *The high energy demand of neuronal cells caused by passive leak currents is not a waste of energy.* Cell Biochem Biophys, 2013. **67**(2): p. 527-35. DOI: 10.1007/s12013-013-9538-3.
7. Berndt, N., et al., *The influence of the chloride currents on action potential firing and volume regulation of excitable cells studied by a kinetic model.* J Theor Biol, 2011. **276**(1): p. 42-9. DOI: 10.1016/j.jtbi.2011.01.022.
8. Crambert, G., et al., *Transport and pharmacological properties of nine different human Na,K-ATPase isozymes.* Journal of Biological Chemistry, 2000. **275**(3): p. 1976-1986. DOI: DOI 10.1074/jbc.275.3.1976.
9. DiFranco, M., et al., *Na,K-ATPase alpha2 activity in mammalian skeletal muscle T-tubules is acutely stimulated by extracellular K+.* J Gen Physiol, 2015. **146**(4): p. 281-94. DOI: 10.1085/jgp.201511407.
10. Armstrong, C.M., *The Na/K pump, Cl ion, and osmotic stabilization of cells.* Proc Natl Acad Sci U S A, 2003. **100**(10): p. 6257-62. DOI: 10.1073/pnas.0931278100.
11. Hodgkin, A.L. and A.F. Huxley, *A quantitative description of membrane current and its application to conduction and excitation in nerve.* J Physiol, 1952. **117**(4): p. 500-44. DOI: 10.1113/jphysiol.1952.sp004764.
12. Kager, H., W.J. Wadman, and G.G. Somjen, *Seizure-like afterdischarges simulated in a model neuron.* J Comput Neurosci, 2007. **22**(2): p. 105-28. DOI: 10.1007/s10827-006-0001-y.
13. Hodgkin, A.L. and P. Horowicz, *The influence of potassium and chloride ions on the membrane potential of single muscle fibres.* J Physiol, 1959. **148**: p. 127-60. DOI: 10.1113/jphysiol.1959.sp006278.
14. Frankenhaeuser, B. and A.F. Huxley, *The Action Potential in the Myelinated Nerve Fiber of Xenopus Laevis as Computed on the Basis of Voltage Clamp Data.* J Physiol, 1964. **171**: p. 302-15. DOI: 10.1113/jphysiol.1964.sp007378.